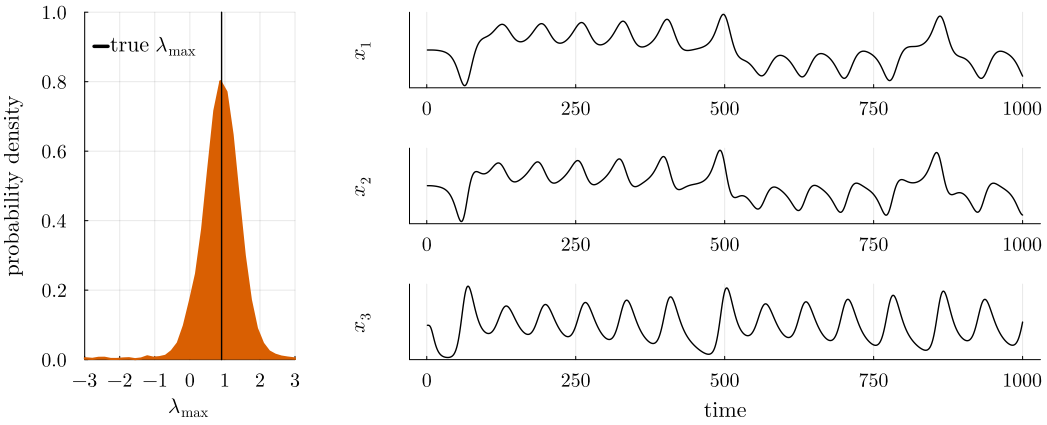

Figure 1: **Left:** Black line denotes the known maximum Lyapunov exponent λ_{max} of the Lorenz system ($\lambda_{max} \approx 0.9056$; [2]). In orange is the probability density over maximal λ_{max} values assessed on 1000 convSSMs inferred from $n = 10$ time series sampled from the Lorenz system (100 models per time series), convolved with the hemodynamic response function (settings: $TR = 0.5$, time series length $T = 1000$). The inferred λ_{max} center narrowly around the true values. **Right:** Example of one time series used for inference, where x_1 (top), x_2 (middle), and x_3 (bottom) Lorenz dimensions are displayed. This limited information suffices to infer an unbiased $\hat{\lambda}_{max}$ with high precision.

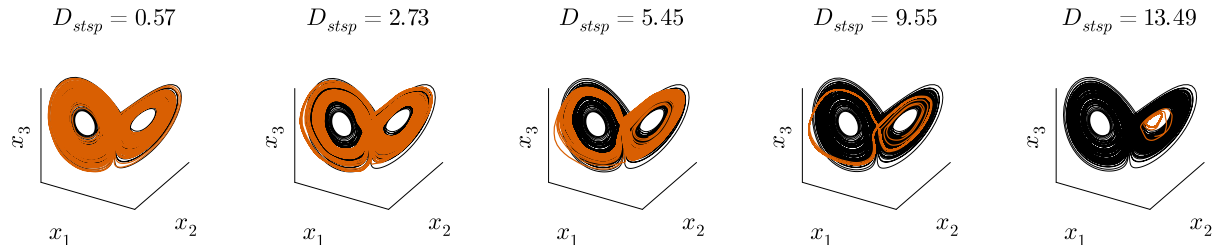

Figure 2: Illustration of reconstruction performance as a function of performance measure D_{stsp}. As D_{stsp} increases, the attractor overlap decreases. At an absolute value of around $D_{stsp} \approx 9$, the reconstructed attractor is still chaotic but does not precisely overlap anymore, while at larger values, k-cycles emerge. Notice that average D_{stsp} reconstruction values for the convSSM were $D_{stsp} < 0.30$ at noise level $\sigma = .01$ and $D_{stsp} < 0.71$ at noise level $\sigma = .1$, indicating successful reconstructions in a large proportion of estimates.

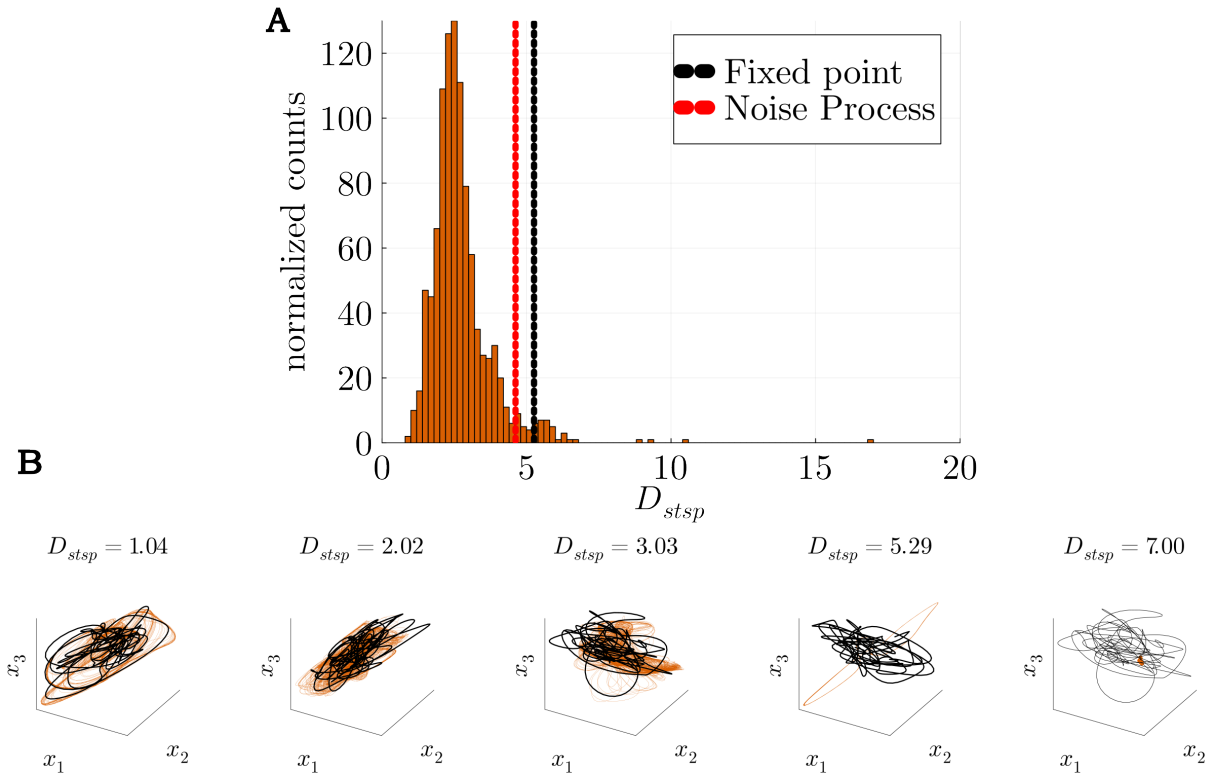

Figure 3: **A:** Distribution over D_{stsp} for $n = 1020$ systems inferred with the convSSM on the empirical LEMON data set. Dotted lines indicate comparison thresholds generated by a fixed point (black dotted line) where all mass is centered on the mean of the data, and a Gaussian white noise process (red dotted line), where points are drawn from a Gaussian with mean and variance equal to the data. **B:** Illustration of reconstruction performance as a function of performance measure D_{stsp}. At an absolute value of D_{stsp} around the noise process threshold, trained systems start exhibiting poor overlap, e.g., by falling into k-cycles inconsistent with the data (second to right panel), or converging into a fixed point (right panel).

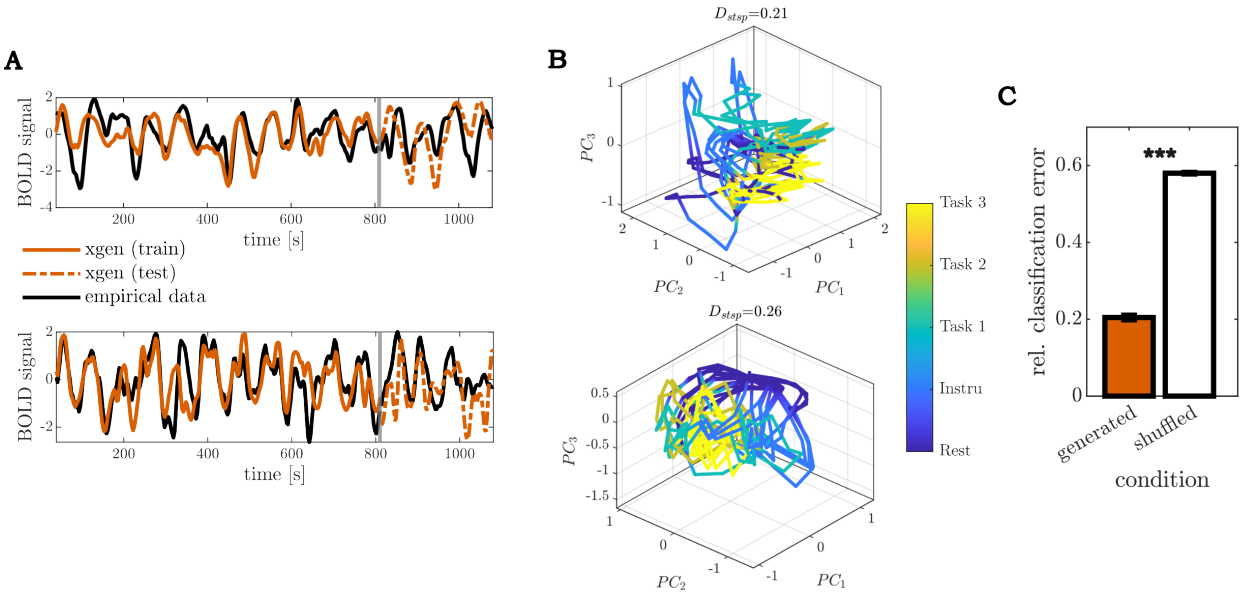

Figure 4: Analysis of additional short ($T = 360$, $TR = 3$) empirical data set of 26 participants (consisting of $N = 20$ time series of working memory related brain regions each). In this experiment, participants repeatedly face three cognitive tasks in a blocked design (a choice reaction task, a continuous delayed response task, and a continuous matching task, see details in [1]). A resting phase and an instruction period precede each task block. Importantly, in all task blocks, the same experimental stimuli are displayed (a sequence of triangles and squares), such that task blocks only differ in the preceding cognitive task instruction and the required cognitive demands. We thus modeled experimental stimuli as (binary) event-related inputs, and the resting and instruction blocks as blocked inputs. Notice, we are thereby explicitly not informing the models of the presented tasks since stimuli are the same across tasks. **A:** Empirical time series of the left parietal cortex (black) of two participants, and model-generated time series on the training set (orange straight line), and the test set (orange dotted line) are displayed. **B:** Generated state space trajectories of the corresponding models in **A**, projected onto the first three principle components (PCs), color-coded by experimental stages (colorbar). **C:** Classification error (y-axis) obtained by classifying the five task stages (see colorbar in **B**) on the generated latent trajectories of the out-of-sample test set using a linear discriminant analysis. The classification error is lower for the convSSM (orange bar) than when compared to a control condition in which the generated trajectories are shuffled in time (white bar; $T(25) = 59.40, p < .001$). For the analysis, we inferred 20 convSSM models on the first 270 time points of each participant, and then forecasted the next 90 time points (test set). Error was assessed by averaging across all 20 models per participant. Mean and SEM are displayed.

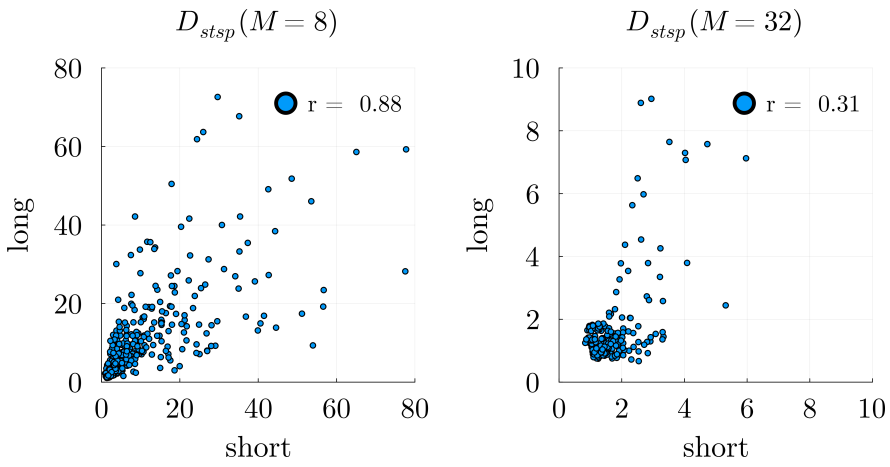

Figure 5: Correlations in D_{stsp} assessed on short and long ALN data sets, for different numbers of dimensions M of the latent model, using an approach where only M units are tied to the N observations, at fixed observation dimensions $N = 16$. **Left:** $M < N$ for $M = 8$ (610 data points). **Right:** $M > N$ with $M = 32$ (240 data points). Both correlations are significant at $p < .001$.

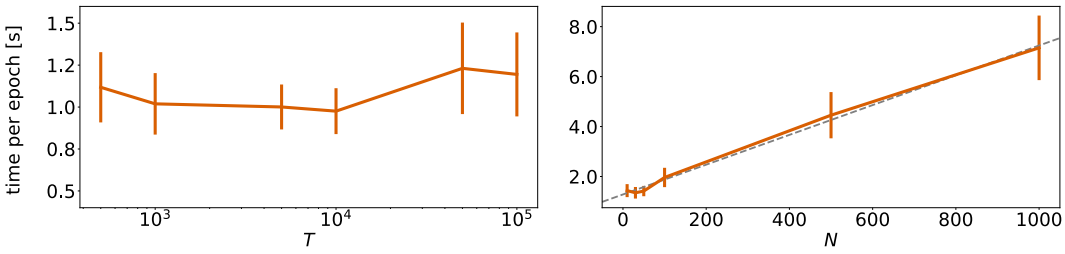

Figure 6: **Left:** Training duration per epoch ($y - axis$) in seconds for different time series length T ($x - axis$), and **right:** observation dimension N ($x - axis$). Grey dashed line indicates linear curve fit, that is, a linear scaling with N. Mean and standard error are displayed.

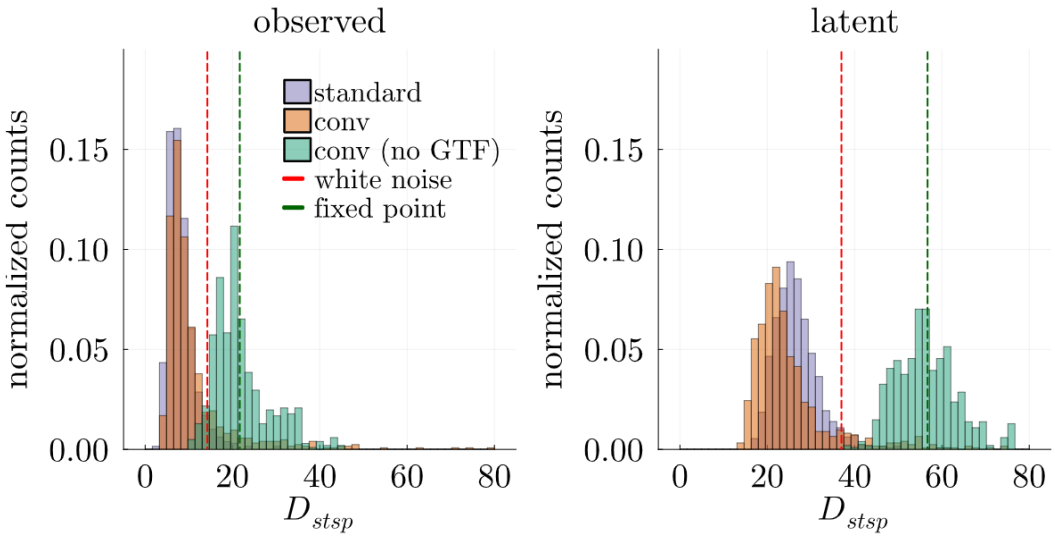

Figure 7: Comparison of standard SSM ('standard'; $N = 790$ models), convSSM ('conv'; $N = 770$ models), and convSSM trained without generalized teacher forcing ('conv (NoGTF)'; $N = 620$ models) on the ALN data set. Histograms over D_{stsp} assessed on the observed space (**left panel**) and latent dynamical system (DS) space (**right panel**) are displayed. The convSSM outperforms the standard SSM in latent space (rank-sum test $Z = 10.19$, $p < .001$), demonstrating a better recovery of the ground truth DS. Red dashed line indicates the average D_{stsp} obtained when drawing from a Gaussian white noise distribution with mean and variance equal to the time series. Green dashed line indicates the average D_{stsp} obtained when all mass is centered on the average value (akin to a fixed point).

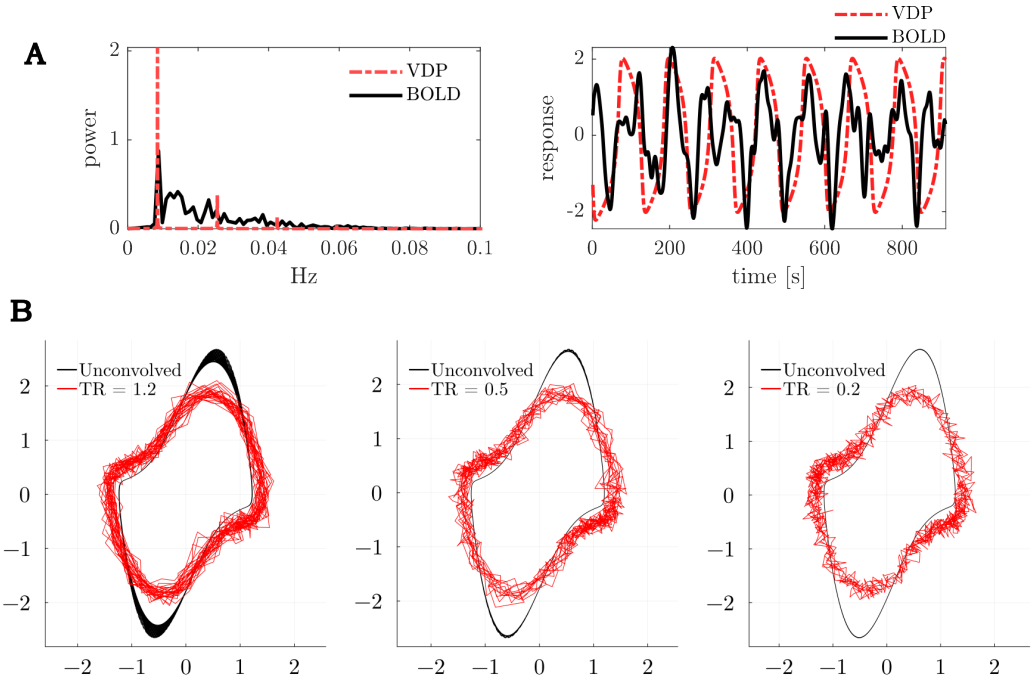

Figure 8: Illustration of additional van der Pol (VDP) oscillator benchmark. **A:** VDP oscillator was tuned to the power spectrum of the empirical BOLD signal as illustrated here (left: power spectrum, and right: one dimension of the VDP oscillator in red superimposed on an empirical time series). For the analyses, we tuned the VDP to each sampling frequency separately. **B:** Examples of VDP time series samples at $TR = 1.2$ (left), $TR = 0.5$ (middle), and $TR = 0.2$ (right) at noise $\sigma = 0.1$ and used for training.

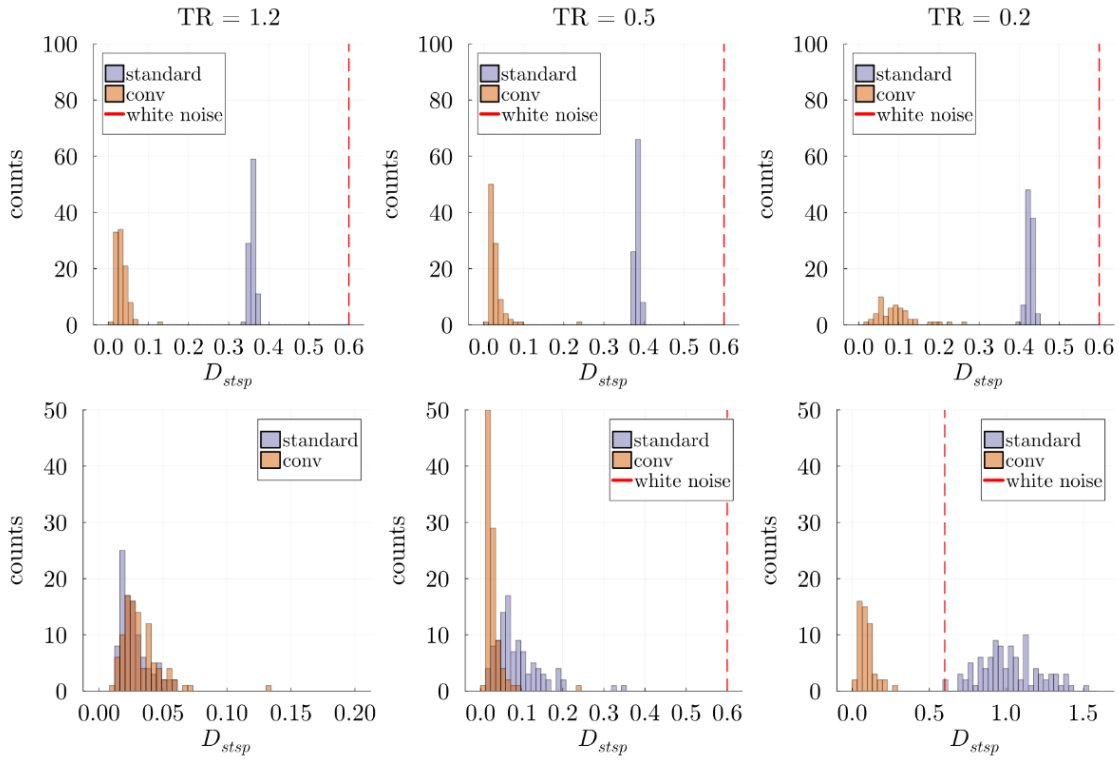

Figure 9: Comparison of standard SSM ('standard') and convSSM ('conv') on the van der Pol oscillator (see Figure 8). **Top:** Histograms over D_{stsp} assessed on the generated latent trajectories of 100 convSSMs and standard SSMs trained on noisy van der Pol time series ($T = 1000$, noise $\sigma = 0.1$), convolved with a $TR = 1.2$ (left panel), $TR = 0.5$ (middle panel), and $TR = 0.2$ (right panel). **Bottom:** Same for D_{stsp} assessed after deconvolving the states of the standard SSM (with minimum noise level $\tilde{\sigma}_{min} = 0.0001$). Red dotted line marks a white noise reference point.

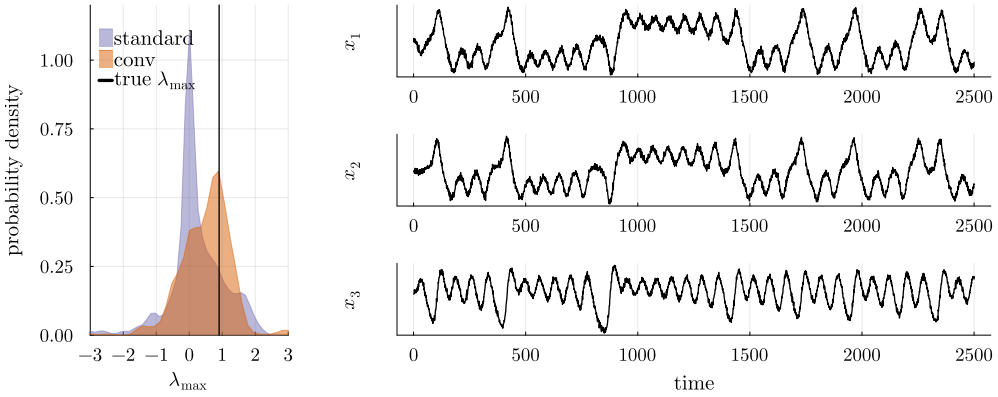

Figure 10: **Left:** Black line denotes the known maximum Lyapunov exponent λ_{max} of the Lorenz system ($\lambda_{max} \approx 0.9056$). Probability densities for λ_{max} values assessed on convSSMs (orange), and standard SSMs (blue) are displayed. 100 systems were inferred on $N = 10$ time series (10 systems per time series) sampled from the Lorenz system, convolved with the hemodynamic response function (settings: $TR = 0.2$, time series length $T = 2500$, noise $\sigma = 0.1$). convSSMs and standard SSMs were inferred with the same number of parameters and time series used for training were identical. The inferred $\hat{\lambda}_{max}$ center narrowly around the true λ_{max} for the convSSM. The standard SSM in contrast is strongly biased. **Right:** Example of one time series used for inference, where x_1 (top), x_2 (middle), and x_3 (bottom) Lorenz dimensions are displayed.

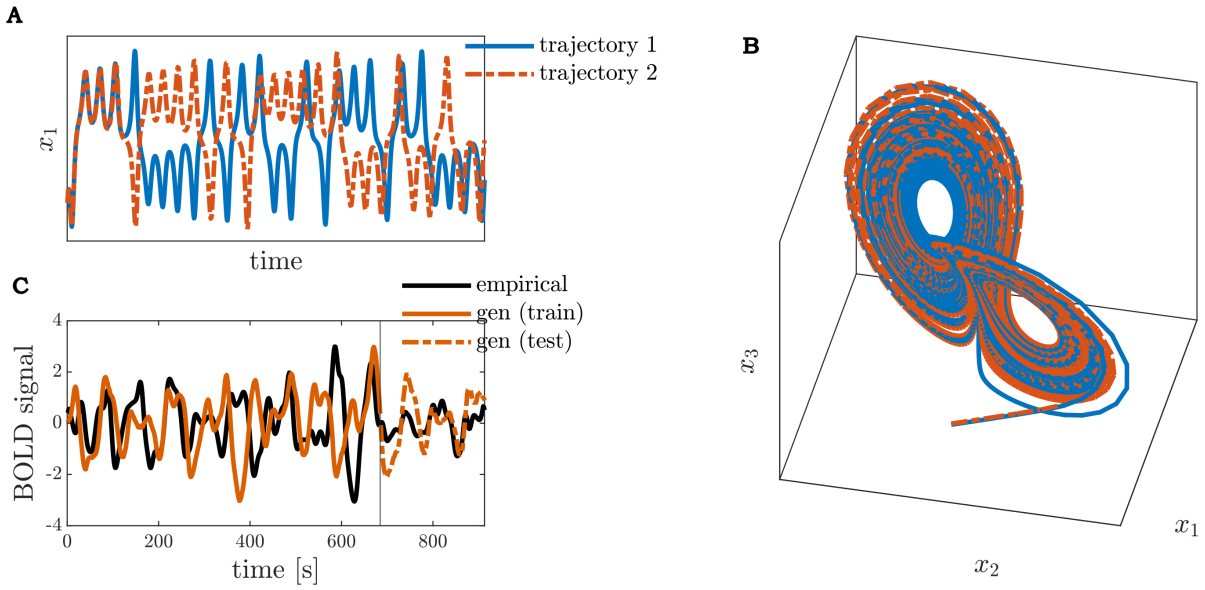

Figure 11: **A:** Two trajectories (red and blue) sampled from the Lorenz system in the chaotic regime at close to identical initial conditions (x_1-component of Lorenz system is displayed). After a short initial period of temporal overlap, the trajectories diverge. **B:** Same trajectories displayed in state space. Although trajectories do not overlap in time, they overlap in space, within the boundaries of the chaotic attractor. **C:** Empirical time series obtained the LEMON data set (black), and a convSSM-generated time series (orange), with positive maximum Lyapunov exponent, i.e., a chaotic system). After a short initial overlap, trajectories diverge. Notice also that before the convSSM makes its first prediction, it runs for l =length(HRF) time steps (until it can be fully convolved with the HRF), plenty of time to diverge before the visualization.

Table 1: DSR measures evaluated for the convSSM, standard SSM, ConvSSM trained without generalized teacher forcing by setting $\alpha = 0$ (ConvSSM-NoGTV, so far evaluated on 10/50 participants), and MINDy, trained on the empirical LEMON dataset. Model runs were excluded if the 1-step PE > 1.

metric	ConvSSM	LinSSM	No TF ($\alpha = 0$)	MINDy	Noise process	Fixed point
D_{stsp}	2.73 ± 1.09	2.77 ± 0.93	5.41 ± 0.86	6.79 ± 1.92	4.62 ± 0.91	5.27 ± 1.27
D_{PSE}	0.14 ± 0.03	0.15 ± 0.03	0.32 ± 0.07	0.27 ± 0.06	0.76 ± 0.02	-
1-step PE	0.17 ± 0.33	0.12 ± 0.04	0.58 ± 0.32	0.956 ± 0.135	-	-
5-step PE	0.54 ± 0.26	0.42 ± 0.09	1.05 ± 0.17	1.62 ± 0.23	-	-
10-step PE	1.78 ± 0.38	2.00 ± 0.44	1.34 ± 0.18	1.97 ± 0.31	-	-

Algorithm 1 Deconvolution in convSSM

Input:

$\mathcal{X}$: measured time series as $(N \times T)$ matrix

Parameters:

ψ: analyzing wavelet

$\tilde{\sigma}_{min}$: minimum noise level

cut_l, cut_r: edge cutoffs

hrf_t: kernel of hemodynamic response function

Output:

$\mathcal{X}_{deconv}$: deconvolved time series as $(N \times T)$ matrix

Initialize $\mathcal{X}_{deconv} :=$ zeros (N, T)
for $i = 1$ **to** N **do**
  $x_t := \mathcal{X}[i, :]$
  $\tilde{\sigma}, \tilde{z}_t :=$ VISUSHRINK(x_t, ψ)
  if $\tilde{\sigma} < \tilde{\sigma}_{min}$ **then**
    $\tilde{\sigma} := \tilde{\sigma}_{min}$
  end if

  Compute Fourier transforms $\mathcal{F}\{\cdot\}$ *and expectation values of spectral densities* $\mathbb{E}\left[|\mathcal{F}\{\cdot\}|^2\right]$
  $X_k := \mathcal{F}\{x_t\}$
  $HRF_k := \mathcal{F}\{hrf_t\}$
  $N_k := \mathbb{E}\left[|\mathcal{F}\{\eta_t\}|^2\right]$
  $S_k := \mathbb{E}\left[|\mathcal{F}\{\tilde{z}_t\}|^2\right]$

  Compute and apply Wiener filter
  $W_k := \frac{HRF_k^* \cdot S_k}{|HRF_k|^2 \cdot S_k + N_k}$
  $\tilde{Z}_k := W_k \cdot X_k$

  Transform back to time domain
  $\tilde{x}_t := \mathcal{F}^{-1}\left\{\tilde{Z}_k\right\}$

  Remove signal edges
  $\tilde{x}_t[\text{begin} + cut_l : \text{end}] :=$ NaN
  $\tilde{x}_t[\text{begin} : \text{end} - cut_r] :=$ NaN
  $\mathcal{X}_{deconv}[i, :] := \tilde{x}_t$
end for

References

[1] G. Koppe, H. Gruppe, G. Sammer, B. Gallhofer, P. Kirsch, and S. Lis. Temporal unpredictability of a stimulus sequence affects brain activation differently depending on cognitive task demands. *Neuroimage*, 101:236–244, 2014.

[2] D. Viswanath. *Lyapunov exponents from random Fibonacci sequences to the Lorenz equations*. Cornell University, 1998.